



HAL
open science

Phase Variation of Ingestible Dipole, Loop, and Patch Antennas in Gastrointestinal Tract

Erdem Cil, Denys Nikolayev

► **To cite this version:**

Erdem Cil, Denys Nikolayev. Phase Variation of Ingestible Dipole, Loop, and Patch Antennas in Gastrointestinal Tract. 2024 18th European Conference on Antennas and Propagation (EuCAP), Mar 2024, Glasgow, United Kingdom. 10.23919/eucap60739.2024.10501272 . hal-04566641

HAL Id: hal-04566641

<https://hal.science/hal-04566641v1>

Submitted on 11 Jul 2024

HAL is a multi-disciplinary open access archive for the deposit and dissemination of scientific research documents, whether they are published or not. The documents may come from teaching and research institutions in France or abroad, or from public or private research centers.

L'archive ouverte pluridisciplinaire **HAL**, est destinée au dépôt et à la diffusion de documents scientifiques de niveau recherche, publiés ou non, émanant des établissements d'enseignement et de recherche français ou étrangers, des laboratoires publics ou privés.

Phase Variation of Ingestible Dipole, Loop, and Patch Antennas in Gastrointestinal Tract

Erdem Cil^{*†} and Denys Nikolayev^{*}

^{*}IETR (l'Institut d'électronique et des technologies du numérique) UMR 6164, CNRS / Univ. Rennes, Rennes, France

[†]BodyCAP, Héraultville-Saint-Clair, France

erdem.cil@univ-rennes.fr; denys.nikolayev@deniq.com

Abstract—Ingestible and implantable antennas are widely used in current in-body bioelectronic devices. This paper aims to examine the behavior of magnitude and phase of the reflection coefficient of ingestible antennas in the gastrointestinal tract for the purpose of sensing and distinguishing the gastrointestinal tissues (stomach, small intestine, and large intestine). In this context, the paper presents the changes in these parameters for three common antenna types (dipole, loop, and patch) in the interval of electromagnetic properties (relative permittivity and electrical conductivity) of the gastrointestinal tissues. The antennas operate in the 433 MHz Industrial, Scientific, and Medical Band and conform to the inner surface of polylactic-acid capsules with shell thicknesses of 0.2, 0.5, and 1 mm. They are optimized in a homogeneous spherical phantom having time-averaged electromagnetic properties of the gastrointestinal tissues. The changes in the magnitude and phase are presented in the intervals of 57–72 for the relative permittivity and 0.5–2.1 S/m for the conductivity, covering the values of the gastrointestinal tissues. The results show that the phase varies in wider intervals than the magnitude, mostly due to the changes in the conductivity, indicating that it is better to track the phase for distinguishing the gastrointestinal tissues.

Index Terms—Antenna impedance, conformal antennas, in-body antennas, ingestible devices, wireless bioelectronics.

I. INTRODUCTION

In recent years, the number of wireless biomedical devices used in health-related sensing applications has greatly increased. Implantable and ingestible bioelectronics are among medical devices that operate inside of the body and can be implemented to sense and actuate physiological parameters of humans [1], [2] and animals [3]. Different application fields of bio-sensing devices include, for example, endoscopy [4]–[6], neuro-recording [7], [8], and vascular blood flow sensing [9], [10].

In-body bioelectronics devices require several components that must be integrated inside a small area to achieve their task effectively [11]. Among these components, the implantable or ingestible antenna has a crucial role not only in the communication but also in the sensing performance of the entire system, and meticulous design of such multiplexed sensor–antenna can significantly improve the overall performance of the device in terms of both sensing and radiation performance [12]–[14]. Various types of multiplexed biosensor antennas such as helix [9], multiple-input-multiple-output (MIMO) [15], and loop antennas [16] have been proposed for in-body applications.

One of the antenna parameters that is frequently tracked in biosensing applications is the reflection coefficient (in particular, the resonant frequency) of the in-body antenna, as in [17] and [18]. The reflection coefficient is tracked mostly in the cases where it is likely to observe a change in the electromagnetic (EM) properties (relative permittivity, ϵ_r , and electrical conductivity, σ) of the environment, which is the subject of sensing, as these properties affect the reflection coefficient. One of the biological environments where this methodology can be employed is the gastrointestinal (GI) tract. The GI tissues (stomach, small intestine, and large intestine) have varying and nondeterministic EM properties [19], which leads to changes in the reflection coefficient (both in magnitude and in phase) of a capsule-integrated ingestible antenna as the capsule advances through the GI tract. By tracking these changes, it can be possible to sense and distinguish the GI tissues from each other and to locate the capsule inside the GI tract in real-time, which can help identify specific pathologies such as gastroparesis [20].

In this context, this paper examines the effect of a range of EM properties encountered in the GI tissues on the magnitude and the phase of the reflection coefficient of ingestible antennas using three types of typical antennas (dipole, loop, and patch). The main focus of the paper is to examine the phase; however, magnitude variations are also presented for the sake of completeness. The paper also aims to determine which of these two parameters is better to track for distinguishing the GI tissues. The results presented in this paper can be considered as a guideline for designing antennas with sensing functionalities in the GI tract.

II. ANTENNA MODELS AND SIMULATION SETUP

Three antenna models that were previously designed by the authors are used for the examination in this paper: the dipole, the loop, and the patch antenna shown in Fig. 1. The dipole and the loop are meandered antennas, and the details for their design can be found in [20] and [21]. The patch antenna consists of two identical radiating elements having stepped transition that are connected to each other with a meandered microstrip line. This antenna is explained in detail in [22]. The antennas are designed on a 20 mm × 54 mm 127- μ m-thick Rogers 5880 substrate ($\epsilon_r = 2.2$, [23]) and conform to the inner surface of polylactic-acid (PLA, $\epsilon_r = 2.7$) capsules as seen in Fig. 2. They are optimized using CST Studio

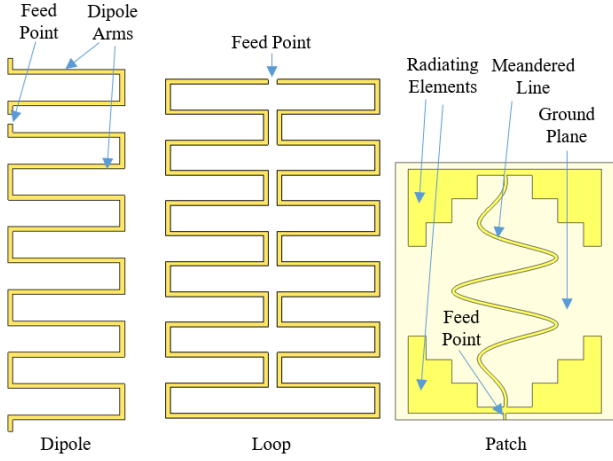


Fig. 1. Models of the dipole, loop, and patch antenna used for the examination.

TABLE I
OPTIMIZED VALUES OF PARAMETRIZED DIMENSIONS FOR DIPOLE AND LOOP ANTENNAS

	t (mm)	Length (mm)	Width (mm)	Trace Width (mm)	Feed Offset (mm)	N
Dipole	0.2		14.1			
	0.5	1.9	17.4	0.25	6.6	6
	1		20.35			
Loop	0.2	14.4	1.95			6
	0.5	13.9	1.35	0.25	*	9
	1	14.3	1			13

Suite (Dassault Systèmes Simulia Corp.) to operate in the 433 MHz Industrial, Scientific, and Medical (ISM) Band for three different shell thicknesses ($t = 0.2, 0.5, \text{ and } 1 \text{ mm}$) in a spherical homogeneous phantom having time-averaged EM properties of the GI tract ($\epsilon_r = 63$, $\sigma = 1.02 \text{ S/m}$ at 434 MHz, [21]) as visualized in Fig. 2. These three thickness values are selected to show the dependency of the changes on the shell thickness and to provide further insight. The optimized values of parametrized dimensions are tabulated in Table I for dipole and loop antennas and in Table II for patch antennas. Note that the parametrization of the dimensions of the antennas are the same as in reference publications [20]–[22], hence not repeated here.

To observe the effect of the EM properties on the reflection coefficient, the relative permittivity and the conductivity of the phantom are changed separately. The range for the EM properties of the GI tissues at 434 MHz is 62–67.2 for the relative permittivity and 0.87–1.92 S/m for the conductivity [24]. To include possible variations depending on the individual (due to age, sex, etc.), the relative permittivity is varied between 57–72 with increments of 0.5, and the conductivity is varied between 0.5–2.1 S/m with increments of 0.05 S/m. As one of the variables is varied in its interval, the other one is kept constant at its time-averaged value.

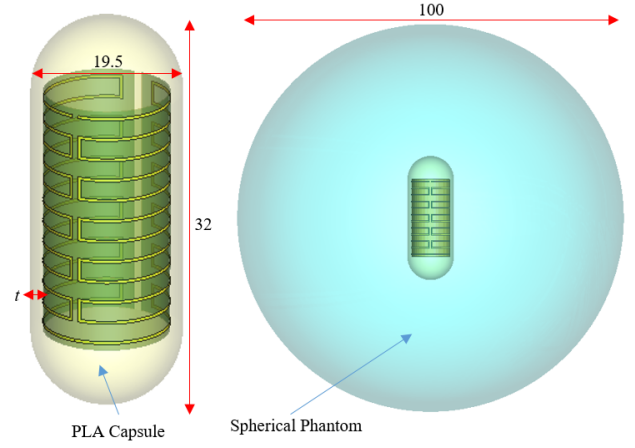


Fig. 2. Loop antenna conforming to the inner surface of the PLA capsule and the capsule placed in the middle of the spherical homogeneous phantom for simulations (units: mm).

TABLE II
OPTIMIZED VALUES OF PARAMETRIZED DIMENSIONS FOR PATCH ANTENNAS

	t (mm)	l_1 (mm)	l_c (mm)	w_1 (mm)	w_2 (mm)	w_c (mm)	w_s (mm)
Patch	0.2	6	1.83	22	0.5	1.99	3.2
	0.5	8.1	2.53	36.5	1.35	4.41	5.9
	1	8.25	2.58	51.2	1.75	6.55	7

III. RESULTS AND DISCUSSION

A. Relative Permittivity

Fig. 3 shows the behaviour of the magnitude and the phase of the reflection coefficient for all antennas in the determined interval of the relative permittivity. It can be seen that the magnitude tends to either monotonically increase or monotonically decrease with increasing relative permittivity for all antennas. The maximum difference in the magnitude is observed for the loop antenna with $t = 0.2 \text{ mm}$ (7.1 dB from $\epsilon_r = 57$ to $\epsilon_r = 72$). As for the phase, the maximum difference is observed for the dipole antenna with $t = 0.2 \text{ mm}$ (43.7° from $\epsilon_r = 57$ to $\epsilon_r = 72$).

B. Electrical Conductivity

Fig. 4 shows the behaviour of the magnitude and the phase of the reflection coefficient for all antennas in the determined interval of the conductivity. It is observed that the magnitude makes a peak at a value in the given interval for all antennas, contrary to the results obtained with the relative permittivity. The maximum difference in the magnitude is observed for the dipole antenna with $t = 0.2 \text{ mm}$ (17.2 dB from $\sigma = 0.7 \text{ S/m}$ to $\sigma = 2.1 \text{ S/m}$). As for the phase, it tends to either monotonically increase or monotonically decrease with increasing conductivity, and the maximum difference is observed for the dipole antenna with $t = 0.2 \text{ mm}$ (163.7° from $\sigma = 0.5 \text{ S/m}$ to $\sigma = 2.1 \text{ S/m}$). It can also be seen that the phase values change in

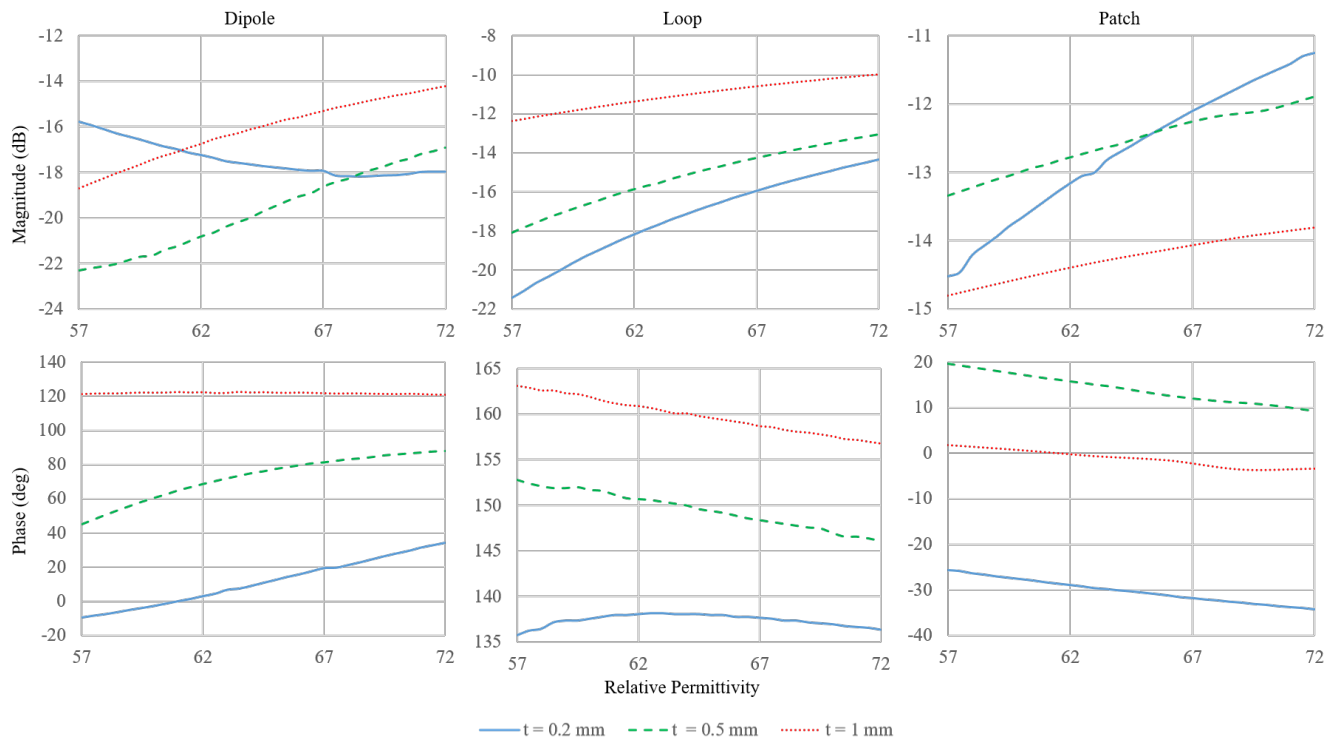


Fig. 3. The effect of the relative permittivity on the magnitude and the phase of the reflection coefficient for dipole, loop, and patch antennas.

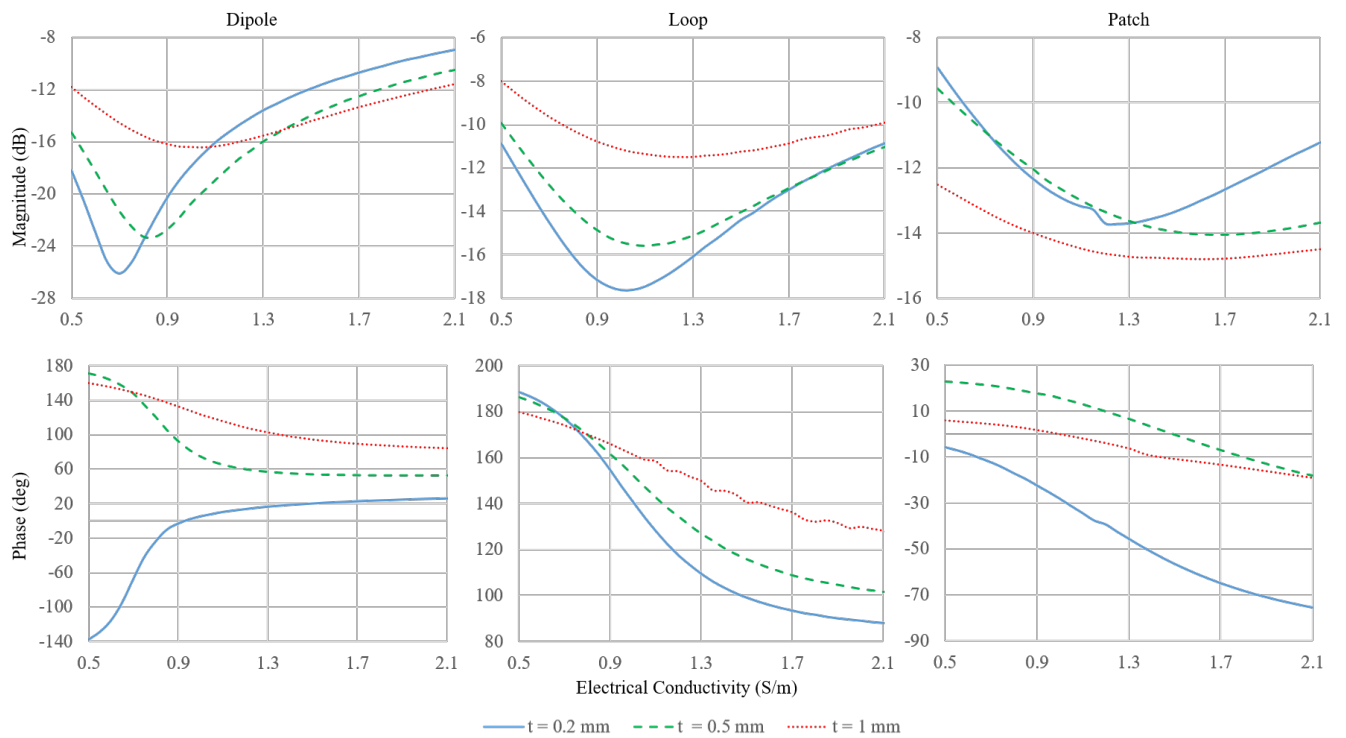


Fig. 4. The effect of the conductivity on the magnitude and the phase of the reflection coefficient for the dipole, loop, and patch antennas.

wider intervals with varying conductivity compared to relative permittivity, indicating that the phase is more susceptible to the changes in the conductivity. Moreover, it is observed that the interval of changes for both magnitude and phase decreases with increasing shell thickness since the fields radiated from the antennas extend less into the tissue.

C. Comments on Sensing Capabilities

From the results in Fig. 3 and Fig. 4, it is observed that the phase values change in wider intervals than the magnitude values. In particular, they change predominantly due to the variations in the conductivity. This shows that it is better to track the changes in phase rather than in magnitude for sensing and distinguishing the GI tissues from each other. In this context, it can be seen that the phase values have the widest interval for dipole antennas. This emphasizes that the dipole antenna is the best option for sensing purposes in the GI tract among these three typical types of antennas. Moreover, the interval of values increases with decreasing shell thickness, indicating that using a thinner shell may increase the sensing capability. However, the designer should keep in mind that decreasing the shell thickness may also decrease the radiation efficiency as the fields radiated from the antenna extend more into the tissues in this case. This is left out of the scope of this paper.

IV. CONCLUSION

This paper examined the behaviour of the reflection coefficient of three common ingestible antenna types in the GI tract with the aim of distinguishing GI tissues from each other. Conformal dipole, loop, and patch antennas operating in the 433 MHz ISM band were simulated in the spherical homogeneous phantom with varying relative permittivity and conductivity. The relative permittivity was changed between 57–72, and the conductivity was changed between 0.5–2.1 S/m. Changes with wider intervals were observed in the phase values, making it a better option to distinguish the GI tissues. Our current work aims at fabrication of the antennas with corresponding RF circuitry [25] and experimental validation in phantoms as well as in animal models for pre-clinical validation. These results will be presented at EuCAP 2024.

ACKNOWLEDGMENT

This work was supported in part by the French *Agence Nationale de la Recherche* (ANR) under grant ANR-21-CE19-0045 (project “MedWave”), in part by Région Bretagne (France) through the *Stratégie d’attractivité durable* (SAD) project “EM-NEURO”, in part by the BodyCAP Company, and in part by the European Regional Development Fund (ERDF) and Région Normandie (France).

REFERENCES

- [1] A. Kiourti and K. S. Nikita, “A review of in-body biotelemetry devices: Implantables, ingestibles, and injectables,” *IEEE Trans. Biomed. Eng.*, vol. 64, no. 7, pp. 1422–1430, 2017.
- [2] A. K. Teshome, B. Kibret, and D. T. H. Lai, “A review of implant communication technology in WBAN: Progress and challenges,” *IEEE Rev. Biomed. Eng.*, vol. 12, pp. 88–99, 2019.
- [3] S. Benaissa *et al.*, “Design and experimental validation of a multiband conformal patch antenna for animal ingestible bolus applications,” *IEEE Trans. Antennas Propag.*, vol. 71, no. 8, pp. 6365–6377, May 2023.
- [4] S. Hayat, S. A. A. Shah, and H. Yoo, “Miniaturized dual-band circularly polarized implantable antenna for capsule endoscopic system,” *IEEE Trans. Antennas Propag.*, 2020.
- [5] M. Suzan Miah, A. N. Khan, C. Icheln, K. Haneda, and K.-I. Takizawa, “Antenna system design for improved wireless capsule endoscope links at 433 MHz,” *IEEE Trans. Antennas Propag.*, vol. 67, no. 4, pp. 2687–2699, 2019.
- [6] J. Wang, M. Leach, E. G. Lim, Z. Wang, R. Pei, and Y. Huang, “An implantable and conformal antenna for wireless capsule endoscopy,” *IEEE Antenn. Wireless Propag. Lett.*, vol. 17, no. 7, pp. 1153–1157, 2018.
- [7] H. Bahrami, A. Mirbozorgi, L. A. Rusch, and B. Gosselin, “Biological channel modeling and implantable UWB antenna design for neural recording systems,” *IEEE Trans. Biomed. Eng.*, vol. 62, no. 1, pp. 88–98, 2015.
- [8] A. Iqbal, M. Al-Hasan, I. B. Mabrouk, and T. A. Denidni, “Simultaneous transmit and receive self-duplexing antenna for head implants,” *IEEE Trans. Antennas Propag.*, vol. 71, no. 11, pp. 8592–8601, 2023.
- [9] Y. Hacohen and S. J. A. Majerus, “A flexible double helix inductive antenna for RFID vascular flow sensing,” *IEEE Sens. J.*, vol. 23, no. 17, pp. 19 044–19 051, 2023.
- [10] J. H. Cheong *et al.*, “An inductively powered implantable blood flow sensor microsystem for vascular grafts,” *IEEE Trans. Biomed. Eng.*, vol. 59, no. 9, pp. 2466–2475, 2012.
- [11] M. R. Yuce and T. Dissanayake, “Easy-to-swallow wireless telemetry,” *IEEE Microw. Mag.*, vol. 13, no. 6, pp. 90–101, 2012.
- [12] A. R. Chishti *et al.*, “Advances in antenna-based techniques for detection and monitoring of critical chronic diseases: A comprehensive review,” *IEEE Access*, vol. 11, pp. 104 463–104 484, 2023.
- [13] D. Nikolayev, W. Joseph, M. Zhadobov, R. Sauleau, and L. Martens, “Optimal radiation of body-implanted capsules,” *Phys. Rev. Letters*, vol. 122, no. 10, p. 108101, Mar. 2019.
- [14] I. V. Soares *et al.*, “Wireless powering efficiency of deep-body implantable devices,” *IEEE Trans. Microw. Theory Techn.*, vol. 71, no. 6, pp. 2680–2692, Jun. 2023.
- [15] A. Iqbal, M. Al-Hasan, I. B. Mabrouk, and T. A. Denidni, “Deep-implanted MIMO antenna sensor for implantable medical devices,” *IEEE Sens. J.*, vol. 23, no. 3, pp. 2105–2112, 2023.
- [16] M. H. Behfar, L. Sydänheimo, S. Roy, and L. Ukkonen, “Dual-port planar antenna for implantable inductively coupled sensors,” *IEEE Trans. Antennas Propag.*, vol. 65, no. 11, pp. 5732–5739, 2017.
- [17] W. Wang *et al.*, “An implantable antenna sensor for medical applications,” *IEEE Sens. J.*, vol. 21, no. 13, pp. 14 035–14 042, 2021.
- [18] M. Manoufali, K. Bialkowski, B. Mohammed, P. C. Mills, and A. M. Abbosh, “Compact implantable antennas for cerebrospinal fluid monitoring,” *IEEE Trans. Antennas Propag.*, vol. 67, no. 8, pp. 4955–4967, 2019.
- [19] Z. Sipus, A. Šušnjara, A. K. Skrivervik, D. Poljak, and M. Bosiljevac, “Influence of uncertainty of body permittivity on achievable radiation efficiency of implantable antennas—Stochastic analysis,” *IEEE Trans. Antennas Propag.*, vol. 69, no. 10, pp. 6894–6905, Oct. 2021.
- [20] E. Cil *et al.*, “On the use of impedance detuning for gastrointestinal segment tracking of ingestible capsules,” *IEEE Trans. Antennas Propag.*, vol. 71, no. 2, pp. 1977–1981, 2023.
- [21] E. Cil, S. Dumanli, and D. Nikolayev, “Examination of impedance response of capsule-integrated antennas through gastrointestinal tract,” in *Proc. 16th Eur. Conf. Antennas Propag. (EuCAP 2022)*, Madrid, Spain, 2022, pp. 1–5.
- [22] D. Nikolayev, W. Joseph, A. Skrivervik, M. Zhadobov, L. Martens, and R. Sauleau, “Dielectric-loaded conformal microstrip antennas for versatile in-body applications,” *IEEE Antenn. Wireless Propag. Lett.*, vol. 18, no. 12, pp. 2686–2690, 2019.
- [23] *Rogers Corporation*, October 2023. [Online]. Available: <https://www.rogerscorp.com/>
- [24] S. Gabriel, R. W. Lau, and C. Gabriel, “The dielectric properties of biological tissues: II. Measurements in the frequency range 10 Hz to 20 GHz,” *Phys. Med. Biol.*, vol. 41, pp. 2251–2269, 1996.
- [25] D. Nikolayev, “Biotelemetry device that can be ingested and implanted *in vivo*,” US Patent US20 210 030 305A1, Feb., 2021.